

# 3D multi-scale modeling of mortar mechanical behavior and effects of microstructural changes

F. Bernard, S. Kamali-Bernard, W. Prince & M. Hjjaj  
*INSA, Rennes, France*

**ABSTRACT:** A 3D numerical modeling of mortar at the micro and meso-level is presented. Two numerical tools are combined to predict mechanical behavior of mortar. An explicit digital microstructure of a portland cement paste containing the different phases is obtained using NIST's CEMHYD3D and starting from the mineralogical composition of the cement and water-to-cement ratio. An explicit digital meso-structure of a mortar is also obtained using CEMHYD3D and considering it as a heterogeneous material composed of sand particles embedded in a hardened cement paste. The 3D pixelized images are then converted to Finite Elements meshes compatible with the FE software Abaqus. This code is then used to predict the mechanical behavior at the different scales. The outcomes of the simulation at the micro-scale are used at the meso-level modeling. This approach is then applied to investigate the durability and the mechanical behavior evolution of concrete structures submitted to leaching by water.

## 1 INTRODUCTION

Concrete is a highly heterogeneous material at the different observation scales. Three elementary levels of heterogeneity can be considered.

- On the macro-scale, large aggregates with Interfacial Transition Zone (ITZ) embedded in a matrix of mortar can typically be observed.
- This mortar consists of small sand particles bonded by cement paste. At this scale, called hereafter meso-level or meso-scale, air voids are generally observed too.
- Finally, the micro-level is the scale of the hydrated cement paste. This paste is a heterogeneous and complex pore medium in which the main solid phases are Calcium Silicate Hydrates (C-S-H), Portlandite (Calcium Hydroxides or CH) and hydrated aluminates and sulfoaluminates phases. The solid phases are in chemical equilibrium with an interstitial solution that partially or totally fills the porosity.

Besides all these various constituents summarized above, the differences in properties of the various constituents at the different scales further increase the heterogeneity of cement-based materials. Variation in stiffness and strength of the components has influence on the global stiffness and fracture behavior of the material.

The tremendous increase of computational capabilities has strongly favored the development of

numerical simulation based on a more realistic explicit description of microstructure (Cailletaud 2000). Using such computational approaches has many advantages compared to more traditional methods, among them:

- the understanding of local deformation mechanisms, stress concentration and distribution in the constituents of composite materials;
- the finest prediction of the overall properties of heterogeneous materials. Numerical methods are more precise than homogeneous techniques when the properties of the constituents are highly contrasted (like in cement-based materials) and in the case of complex global loading conditions (multiaxial, cyclic behavior...);
- the simulation of local damage processes : the computation of explicit microstructures provides damage initiation which is not driven by mean values of stress and strain in each component. These local data can also be coupled to damage criteria or damage evolution equations to predict initiation and propagation of damage or cracks;
- the taking into account of a microstructure evolution due to chemical reactions in order to study durability problems of concrete for example.

The outcomes of such computational approaches could then be used to derive material properties for modeling concrete as a homogeneous material to analyze structures.

In this paper, the micro-scale of the cement paste and the meso-scale of the mortar are investigated. A multi-scale modeling is proposed to predict the mechanical behavior of the material. Microstructural mechanics generally proceeds in three main steps:

- representation of the micro- and mesostructures in a realistic manner,
- choice of the numerical techniques to solve the boundary value problem,
- and, finally, identification of the constitutive equations of the constituents.

These three steps correspond to the main following parts for each considered scale. Finally the proposed approach is applied to investigate the durability of mortar structures submitted to leaching by water.

## 2 CONSTRUCTION OF THE MICRO- AND MESOSTRUCTURES

The microstructure of cement-based materials is too complex and random to allow for the development of exact analytical formulas that describe how the properties are related to the microstructure. The only real alternative to empirical formulas is to use computer methods.

All simulations presented in this paper are conducted starting from NIST microstructural model (CEMHYD3D). This well-known model has been described in detail elsewhere (Bentz 1997). It is composed of two main programs. First, at the micro-scale the initial non hydrated 3D cement pixelized image is created taking into account the particle size distribution, the randomly arrangement of grains and the mineralogical composition of the considered portland cement as well as the water-to-cement (w/c) ratio. A resolution of  $1 \mu\text{m}/\text{pixel}$  is used.

Then, a cellular-automata based program is used to model the hydration of the initial 3D microstructure and the resulting microstructural development of cement paste. CEMHYD3D allows then the calculation of the various hydrates quantities and of the capillary porosity.

At the meso-scale, mortar is modelled as a continuum of cement paste containing nonoverlapping spherical aggregates following a size distribution corresponding to that of a real mortar. In this study, the first same program as for micro-scale is used to build a 5 mm side elementary cube containing a quantity  $Q_1$  of spheres of diameter  $D_1$ , a quantity  $Q_2$  of spheres of diameter  $D_2$  and a quantity  $Q_3$  of spheres of diameter  $D_3$ . The first spheres represent the grains of sand  $S_1$ , the second, the grains of sand  $S_2$  and the third the air voids. The remaining volume corresponds to the cement paste. ITZ around grains is neglected. The precise mechanical behaviour of this phase needs further research.

However this hypothesis would be more criticable around concrete aggregates at macro-scale.

Figures below show examples of 2D cross sections of microstructures obtained with these tools.

Volume fractions of main components of portland cement paste with w/c=0.4:

Porosity = 17%  
 CH = 14.7%  
 C-S-H = 40.2%  
 $\text{C}_3\text{AH}_6 + \text{AFm} + \text{AFt}$   
 = 17.9%

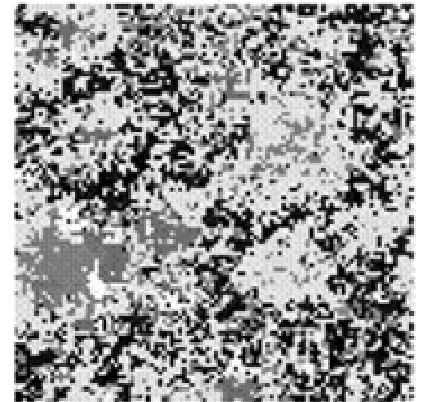


Figure 1. 2D image of the microstructure of hardened cement paste obtained using CEMHYD3D model.

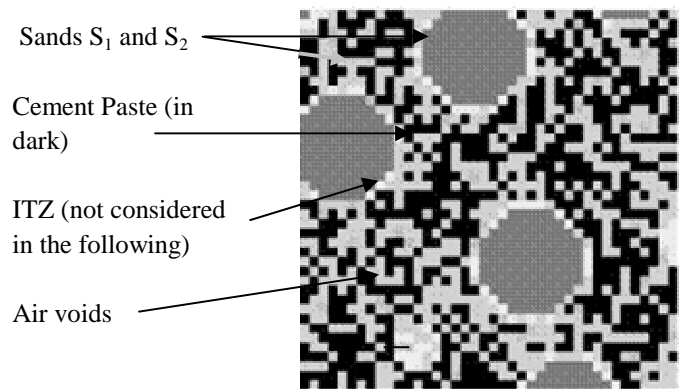


Figure 2. Example of 2D image of the mesostructure of mortar.

The 3D pixelized images obtained in this way should be used by other computer tools such as Finite Elements techniques. Then, in this study, each cubic voxel in the 3D micro- and meso- structures is mapped into a finite element. The FE software used is Abaqus version 6.6.1. The mesh is regular and air voids are explicitly represented but are not meshed. Elementary cubes are respectively  $50 \mu\text{m}$  and  $5 \text{mm}$  side for cement paste and mortar. A finite element has thus a volume equal to  $1 \mu\text{m}^3$  at micro-scale (cube of  $1 \mu\text{m}$  side) and  $125^3 \mu\text{m}^3$  at meso-scale. The length is limited by the memory capacity accorded to the software pre-processor. However, the representativeness of these elementary volumes is verified imposing different boundary conditions (kinematics and stress uniform conditions) according to Kanit (2003).

Then the outcomes of the FE simulation at the micro scale will be used as entry data at the meso-level modeling as follows:

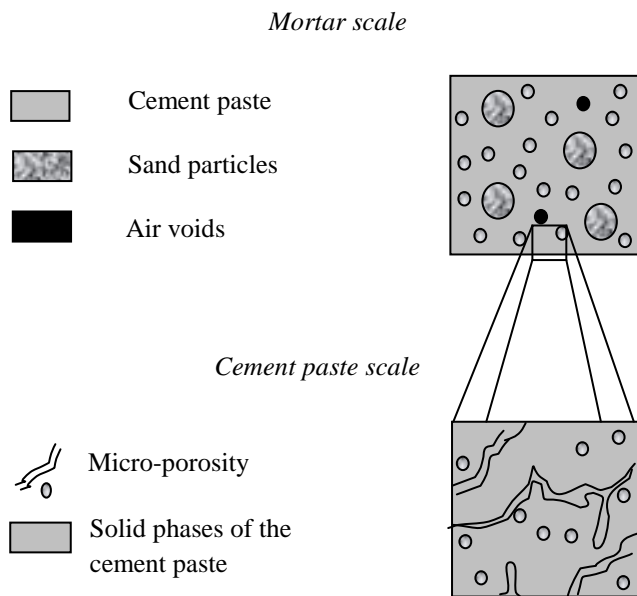


Figure 3. The proposed multi-scale modeling (from cement paste to mortar).

### 3 APPLICATION TO A SPECIFIC MORTAR

#### 3.1 Mortar composition

The mortar modeled in this paper has already been investigated experimentally in Kamali (1999) & Le Bellego (2001). A portland cement is used. Its mineralogy is given below (table 1). The water to cement ratio  $w/c$  is equal to 0.4. These data are used in order to build numerically the hydrated cement paste using CEMHYD3D.

Table 1. Mineralogical composition of Portland cement CEM I 42.5 using Bogue method (% weight content) (Le Bellego 2001).

$C_3S$	$C_2S$	$C_3A$	$C_4AF$	Gypse
53%	19.4%	7.2%	7.9%	5.5%

The studied mortar contains two different sands  $S_1$  and  $S_2$ . The quantities  $Q_1$  and  $Q_2$  are calculated from the mass contents of sands  $S_1$  and  $S_2$  (414  $kg/m^3$  and 966  $kg/m^3$  of mortar).  $D_1$ ,  $D_2$  and  $D_3$  are respectively the average values of the diameters of sands  $S_1$  and  $S_2$  and air voids. They are respectively equal to 1.125 mm, 0.125 mm and 0.375 mm (particle size distributions of sands are not completely known).

The air volume content of the mortar is equal to 3%.

#### 3.2 Modeling at micro-scale (cement paste)

The cement paste corresponding to the considered mortar is modelled. The properties of each phase contained in the cement paste are considered. At this scale, hydrates are supposed to be brittle and

perfectly elastic. The values of the elastic modulus and of the Poisson coefficient of these different phases are issued from the literature (Kamali 2004) and obtained from nano-indentation measurements. The table below presents the values retained in this study.

The tensile strength  $f_t$  is taken proportional to the stiffness values ( $f_t = E/10000$ ). A Rankine criterion is used to model the failure of the different phases. This criterion states that the failure takes place when the maximal principal stress exceeds the tensile strength of the phase.

Table 2. Young's modulus,  $E$ , and Poisson's ratio values of the principal phases used in modeling.

Phases	$E$ (GPa)	$\nu$	References
$C_3S$	117.6	0.314	Boumiz et al. 1997
$C_2S$	117.6	0.314	
$C_3A$	117.6	0.314	
$C_4AF$	117.6	0.314	
Gypsum	45.7	0.33	Choy et al. 1979, Bhalla 1984
Portlandite	42.3	0.324	Monteiro & Chang 1995
C-S-H	22.4	0.25	Damidot et al. 2003
C-S-H <sub>pozz</sub>	22.4	0.25	
AFm	42.3	0.324	
AFt	22.4	0.25	
Empty porosity	0	0	

The aim of the modeling at this scale is to obtain the response of the Representative Elementary Volume (REV) to a tensile solicitation. This outcome is thus obtained in applying a displacement by the Finite Element Method on two opposite faces of the REV. The global effort (sum of the reaction forces at the different nodes) and the total displacement are then compiled and divided respectively by the section surface and the initial length in order to draw the homogenized stress-strain curve. The Poisson coefficient is determined by homogenization of the displacement on the other faces. The simulation is carried out for the considered mortar and results are plotted as shown in figure 4.

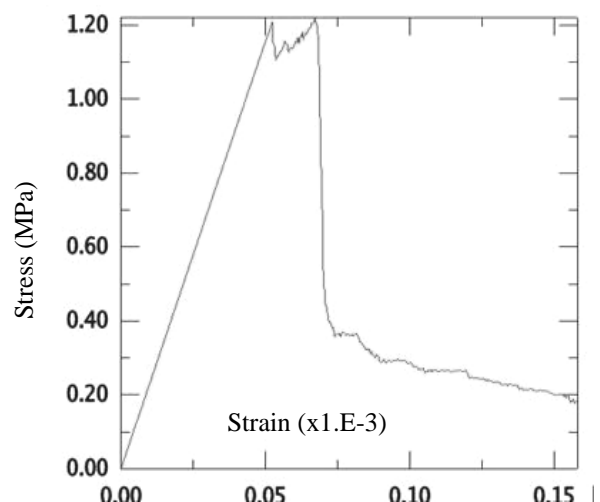


Figure 4. Stress-strain curve in tension for the cement paste corresponding to the considered mortar.

### 3.3 Transfer at meso-scale (mortar)

At the meso-level, a cohesive crack model is used to represent the tensile behavior of hardened cement paste (Hillerborg 1976). Constitutive equations are performed independently at each material point of the Finite Element model. The presence of crack enters into these calculations by the way in which the cracks affect the stress and the material stiffness associated with the material point. Abaqus assumed that cracks are fixed and orthogonal to the direction of the maximum principal stress. A Rankine criterion is used to detect crack initiation. The specification of the post failure tensile behavior needs to enter the post failure stress as a tabular function of displacement across the crack (instead of strain which can introduce mesh sensitivity) (Abaqus 2006). This post failure stress-displacement curve is obtained by inverse identification on simulation of tensile tests performed on a 5 mm side cube of homogeneous hardened cement paste. This side is chosen to be compatible with the displacement needed in the model.

The behavior of the cement paste is plotted in the figure below (Fig. 5). Remaining tensile strength at the end of the test is neglected.

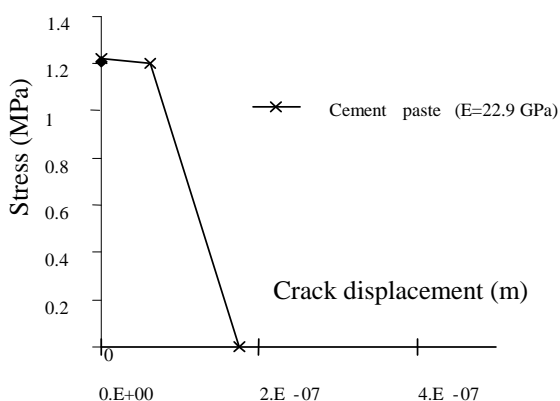


Figure 5. Post Failure stress-displacement curves for the hardened cement paste.

### 3.4 Modeling at meso-scale

At this scale, failure is assumed to be the consequence of crack initiation and propagation at highly localized regions under large tensile stresses concentration. Thus only the tensile behavior of hardened cement paste is needed. Failure in compression is then supposed to be the consequence of tensile eigenstresses resulting from the heterogeneous mesostructure of mortar.

In all the simulations, the cohesive crack model previously identified is imposed to hardened cement paste. Its compressive behavior is assumed to be always linear elastic. As prescribed in Abaqus (Abaqus 2006), in absence of test data, the post cracking shear behavior is assumed to go linearly to zero at the same crack opening displacement used for tension model.

The sand particles are supposed to have the same type of behavior. Their post failure stress-displacement curve is obtained from the value of their fracture energy (120 N/m) (Menou 2004).

In order to help computations and to avoid problems of convergence due to excessive distortion of elements which can no longer carry stress, a brittle failure criterion (“kill-element” technique) is used. Then when the local cracking displacement reaches a critical value, all the stress components are set to zero and the corresponding element is removed from the mesh.

### 3.5 Results of modeling and comparisons with experiments

Figures 6 and 7 show the stress-strain curves obtained in imposing respectively a tensile and a compressive displacement on a Representative Elementary Volume of mortar with free boundary conditions. They also present comparisons between Kamali (1999) & Le Bellego (2001) experiments and the proposed multi-scale modeling.

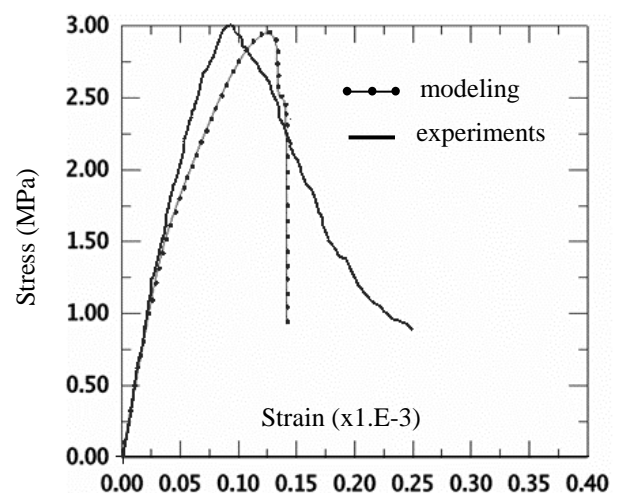


Figure 6. Numerical stress-strain curves in tension for the studied mortar and comparison with experiments.

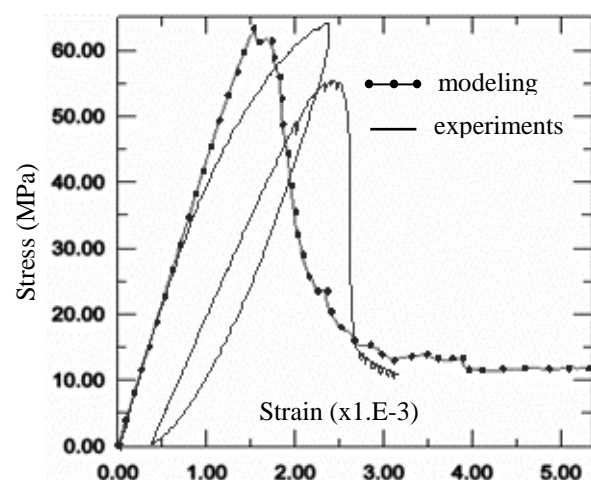


Figure 7. Numerical stress-strain curves in compression for the studied mortar and comparison with experiments.

The experiments were led on 140 mm height and 70 mm diameter samples of mortar. The comparisons show realistic stress-strain responses. Elastic parameters and strength are correctly represented.

For both simulations, non linearities are also well described even if the tensile behavior seems to be a little bit too brittle and if compressive damage evolution before the peak differs slightly from the experiments. However crack patterns before or after the peak are very realistic (failure normal to the solicitation axis in tension and more diffuse with privileged directions parallel to the solicitation axis or making with it an angle of 45° in compression – see Figs. 8 and 9).

The brittle behavior in tension can be explained by the brittle failure criterion which is however interesting for the convergence of the computations.

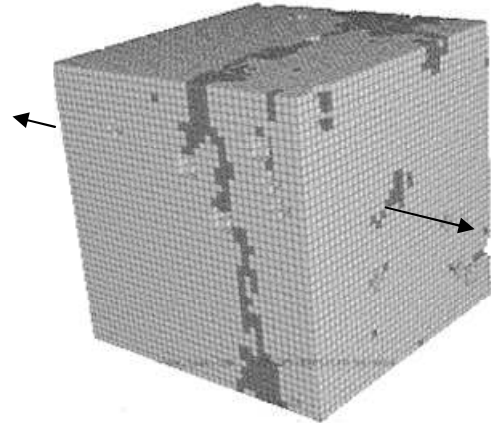


Figure 9. Crack patterns (dark voxels) of the considered mortar obtained by computational calculations in tension.

#### 4 TOWARDS AN APPLICATION TO LEACHING OF CEMENT-BASED MATERIALS

The leaching of cement-based materials is one of the main degradation phenomena taken into account in the design and in the prediction of the service life of concrete structures such as bridges or radioactive waste depositories. The solid phases of the hardened cement paste are in chemical equilibrium with an interstitial solution, which fills the porosity partially or totally. The pH of the pore solution is strongly basic and its value can reach more than 13 in a portland cement paste. When a cement paste is in contact with pure or acid water, ionic transfers occur between the external water and the pore solution of the material. The chemical equilibrium of the paste is then modified and restored by dissolution and/or precipitation of certain hydrates (Adenot 1992). First the Portlandite is dissolved and then the C-S-H are decalcified. This phenomenon is called leaching. The involved degradation is characterized by the presence of several dissolution-precipitation fronts delimiting zones with different physicochemical and mechanical characteristics.

In this paper, the mechanical behavior of the zone without Portlandite is more particularly studied. The effect of the complete leaching of this component is taken into account at the micro-scale in giving to it the properties of the water.

The multi-scale procedure presented previously in paragraph 2 is then applied. The stress-strain curve numerically obtained for a degraded cement paste submitted to a tensile displacement is plotted in figure 10. The identified curve for simulation at meso-scale is also presented in the same figure. The retained crack displacement varies linearly from 0 to  $1.1 \times 10^{-7}$  m.

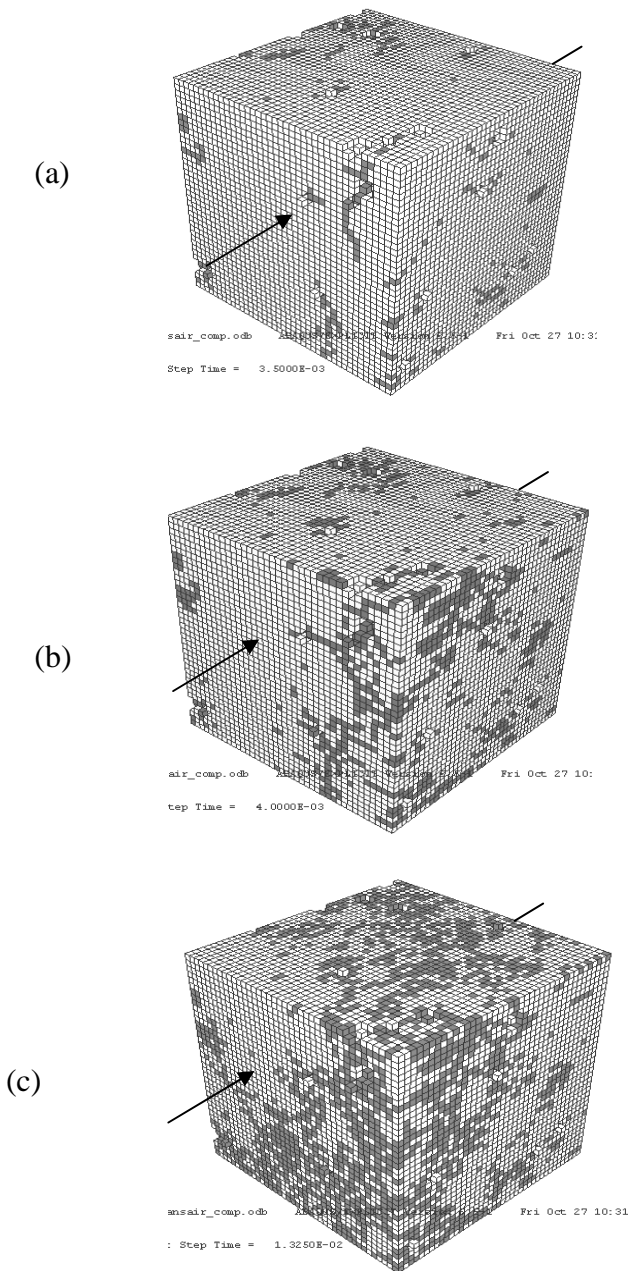


Figure 8. Crack patterns (dark voxels) of the considered mortar obtained by computational calculations in compression (a) before the peak, (b) at the peak, (c) after the peak.

These outcomes are used as entry data at the meso-scale of the mortar.

## 5 CONCLUSION

This work focuses on the use of modern numerical tools as virtual laboratory in order to investigate the mechanical behavior of cement-based materials. 3D simulations at two levels of mortar are presented. The outcome of a lower level (micro-scale) is used as input at a higher level (meso-scale). Two numerical tools are used. First the NIST's 3D model (CEM3D) is used to model a realistic 3D Representative Elementary Volume of cement-based materials at different scales (cement paste and mortar). The pixelized images are converted to Finite Elements Meshes compatible with the FE software Abaqus.

It has been shown that this numerical approach can be successfully used for the prediction of the stress-strain response to compressive and tensile solicitations. Encouraging first results are obtained and modeling is consistent with experimental data. A better knowledge of the properties of hydrates and a more accurate description of the sand (exact particle size description and representation of the Interfacial Transition zone) would allow having better results.

This approach is then applied to investigate the durability of concrete structures submitted to leaching by water. The effect of the dissolution of the Portlandite is investigated and the involving loss of stiffness and strength are estimated.

A following step consists now on applying the proposed approach for the prediction of transport properties (diffusivity and permeability) according to micro- and meso-structures.

## REFERENCES

- Abaqus v.6.6. 2006. Documentation, User's Manual - Part V: Materials.
- Adenot, F. & Buil M. 1992. Modeling of the corrosion of the cement paste by de-ionized water. *Cement and Concrete Research* 22: 489-496.
- Bentz, D.P. 1997. Three-Dimensional Computer simulation of Portland Cement Hydration and Microstructure Development. *Journal of American Ceramic Society* 80 (1): 3-21.
- Bhalla, A.S., Cook, W.R., Hearmon, R.F.S., Jerphagnon, J., Kurtz, S.K., Liu, S.T., Nelson, D.F. & Oudar, J.-L. 1984. *Landolt-Bornstein: Numerical data and functional relationships in science and technology new series*. Group III: Crystal and solid state physics. Volume 18 (Supplement to volume III/11). Elastic, Piezoelectric, Pyroelectric, Piezooptic, Electrooptic Constants, and nonlinear dielectric susceptibilities of crystals. Editors K.-H. Hellwege and A.M. Hellwege. Springer-Verlag Berlin.
- Boumiz, A., Sorrentino, D., Vernet, C. & Tenoudji, F. 1997. Modelling the development of the elastic moduli as a function of the degree of hydration of cement pastes and mortars. *Proceedings 13 of the 2<sup>nd</sup> RILEM Workshop on Hydration and Setting: Why does cement set? An interdisciplinary approach*, Edited by Nonat A. RILEM, Dijon, France.

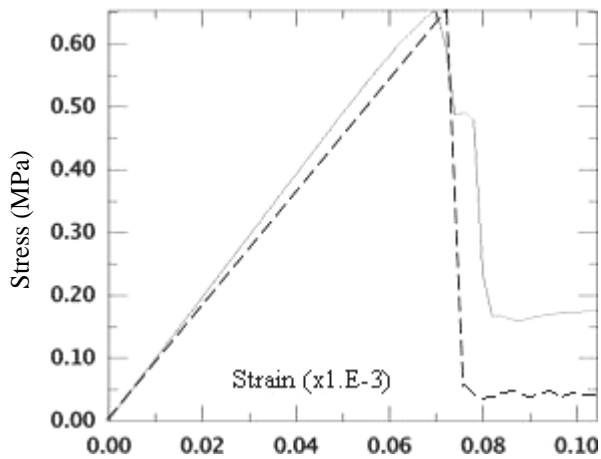


Figure 10. Numerical stress-strain curve in tension for degraded cement paste (dashed curve) and retained identified curve for simulation at meso-scale.

Results of a compressive test on a free boundary mesh of mortar without Portlandite are plotted in figure 11 and compared with the sound mortar. Computational problems of convergence are at the origin of the calculation stop.

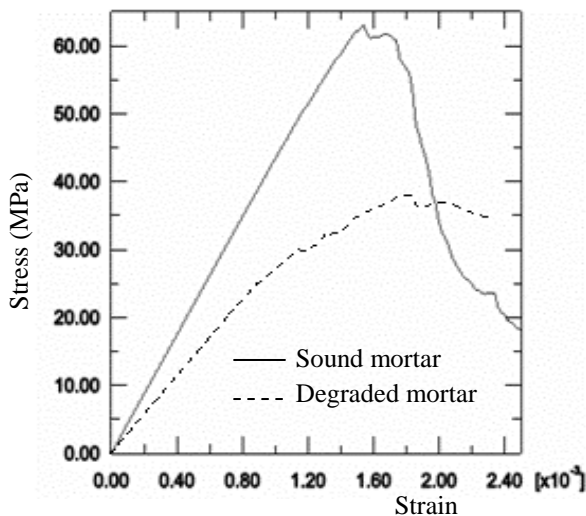


Figure 11. Numerical stress-strain curves in compression for sound and degraded mortar.

Leaching of calcium hydroxides crystals (CH) creates a macro-porosity which has a great effect on the loss of elastic parameters and strength.

A total decrease of the elastic modulus of about 32% (29 GPa versus 42.4 GPa) is obtained. The compressive strength falls from 63 MPa to 38.3 MPa which leads to a decrease of nearly 40%. The degraded mortar presents also a slightly more ductile behavior. All these results seem to be in good agreement with previous experimental studies (Carde 1996, Kamali 1999 & Le Bellego 2001).

- Cailletaud G., Forest S., Jeulin D., Feyel F., Galliet I., Mounoury V. & Quilici S. 2003. Some elements of microstructural mechanics. *Computational Materials Science* 27, Issue 3 : 351-374 .
- Carde, C. 1996. Caractérisation et modélisation de l'altération des propriétés mécaniques due à la lixiviation des matériaux cimentaires. INSA de Toulouse, France. *PhD Thesis*.
- Choy, M.M., Cook, W.R., Hearmon, R.F.S., Jaff, J., Jerphagnon, J., Kurtz, S.K., Liu, S.T. & Nelson, D.F. 1979. *Landolt-Bornstein : Numerical data and functional relationships in science and technology new series*. Group III: Crystal and solid state physics. Volume 11 (Revised and extended edition of volume III/1 and III/2). Elastic, Piezoelectric, Pyroelectric, Piezooptic, Electrooptic constants, and nonlinear dielectric susceptibilities of crystals. Editors K.-H. Kellwege & A.M. Hellwege. Springer-Verlag Berlin.
- Damidot, D., Velez, K. & Sorrentino, F. 2003. Characterisation of interstitial transition zone (ITZ) of high performance cement by nanoindentation technique. presented in the 11<sup>th</sup> *International Congress on the Chemistry of Cement*, Durban.
- Hillerborg, A., Modeer M. & Petersson P.E. 1976. Analysis of Crack Formation and Crack Growth in Concrete by Means of Fracture Mechanics and Finite Elements. *Cement and Concrete Research* 6 : 773–782.
- Kamali, S. 1999. Identification de la loi de comportement mécanique d'un mortier lixivié par du nitrate d'ammonium. Ecole Normale Supérieure de Cachan, France, Rapport de DEA.
- Kamali, S., Moranville, M., Garboczi, Ed., Prene, S. & Gérard, B. 2004. Hydrate dissolution influence on the Young's modulus of cement pastes. *Proceedings of the 5th international conference on fracture mechanics of concrete and concrete structures (FraMCoS)*, Vail, Colorado, 12-16: 631-638.
- Kanit, T., Forest, S., Galliet, I., Mounoury, V. & Jeulin, D. 2003. Determination of the size of the representative volume element for random composites: statistical and numerical approach. *International Journal of Solids and Structures* 40 (13-14): 3647-3679.
- Le Bellégo, C. 2001. Couplage chimie mécanique dans les structures en béton armé attaquées par l'eau – Etude expérimentale et analyse numérique. LMT-ENS de Cachan, France. *PhD Thesis*.
- Menou, A. 2004. Etude du comportement thermomécanique des bétons à haute température : approche multiéchelles de l'endommagement thermique. Université de Pau et des Pays de l'Adour, France. *PhD Thesis*.
- Monteiro, P.J.M. & Chang, C.T. 1995. The elastic moduli of calcium hydroxide. *Cement and Concrete Research* 25: 1605-1609.

## LIST OF SYMBOLS

- C<sub>3</sub>S: tricalcium silicate  
 C<sub>2</sub>S: dicalcium silicate  
 C<sub>3</sub>A: tricalcium aluminate  
 C<sub>4</sub>AF: tetracalcium aluminoferrite  
 C-S-H<sub>pozz</sub>: pozzolanic calcium silicate hydrate  
 AFm: monosulfoaluminate phase  
 AFt: ettringite  
 C<sub>3</sub>AH<sub>6</sub>: hydrogarnet